Global magnetic fluctuations in spheromak plasmas and relaxation toward a minimumenergy state

A. Janos, G. W. Hart, C. H. Nam, and M. Yamada

Citation: Physics of Fluids (1958-1988) **28**, 3667 (1985); doi: 10.1063/1.865321
View online: http://dx.doi.org/10.1063/1.865321
View Table of Contents: http://scitation.aip.org/content/aip/journal/pof1/28/12?ver=pdfcov
Published by the AIP Publishing

Global magnetic fluctuations in spheromak plasmas and relaxation toward a minimum-energy state

A. Janos, G. W. Hart, C. H. Nam, and M. Yamada
Plasma Physics Laboratory, Princeton University, Princeton, New Jersey 08544

(Received 18 April 1985; accepted 5 September 1985)

Globally coherent modes have been observed during formation in the S-1 Spheromak plasma [*Plasma Physics and Controlled Nuclear Fusion 1984* (IAEA, Vienna, Austria, 1985), Vol. 2, p. 535] by analysis of magnetic field fluctuations measured from outside the plasma. The modes are of low n number ($2 \leqslant n \leqslant 5$), where n is defined by the functional dependence $e^{in\phi}$ of the fluctuation on toroidal angle ϕ. These modes are shown to be related to flux conversion and plasma relaxation toward a minimum-energy state during the spheromak formation. The modes are active while the q profile is rapidly changing, with q on axis, q_0, rising to 0.7. A significant finding is the temporal progression through the $n = 5, 4, 3, 2$; $m = 1$ mode sequence as q rises through rational fractions m/n. During formation, peak amplitudes of the $n = 2, 3, 4$ modes relative to the unperturbed field have been observed as high as 20%, while more typical amplitudes are below 5%.

I. INTRODUCTION

Many schemes for the toroidal magnetic confinement of fusion plasmas involve configurations with both poloidal and toroidal fields. Poloidal and toroidal denote the short and long way, respectively, around the torus. The poloidal and toroidal fields of two closely related configurations, the reversed-field pinch[1] (RFP) and the spheromak,[2] are sustained mainly by toroidal and poloidal currents in the plasma. Spheromaks are established without toroidal field coils linking the toroidal plasma, and the toroidal field is maintained entirely by plasma currents. An interesting feature of these two configurations is magnetic flux conversion[3] between the poloidal and toroidal fields. This conversion is important for relaxation of these plasmas toward a stable, minimum-energy Taylor state.[4] Also, sustainment of these discharges is made possible by utilization of this relaxation phenomenon.[5–7] The relaxation process is often accompanied by magnetic field fluctuations,[1,5,8–14] which are thought to be one possible mechanism for the relaxation process. Relaxation in spheromaks was first evidenced by the plasma's maintenance of equilibrium profiles close to the lowest-energy, force-free eigenmodes predicted by theory.[15–17]

In recent S-1 Spheromak experiments,[18,19] flux conversion between the poloidal and toroidal fluxes of the plasma was observed during and after formation of the plasma. Plasmas were observed to adjust themselves during formation such that the ratio of the toroidal plasma current to toroidal magnetic flux in the plasma, I/Φ, was a constant independent of initial conditions such as capacitor bank voltages. The Taylor state is characterized by the force-free condition $\mathbf{j} = \lambda \mathbf{B}$, where λ is a constant independent of position, j is the current density, and B is magnetic field. If λ is constant, then λ also equals I/Φ by simple integration; I/Φ is proportional to the pinch parameter $\theta \equiv 2I/aB_0$ of RFP research through a simple geometric factor involving the plasma size. The time behavior of I/Φ in S-1 was very similar to that of θ in RFP discharges. It was experimentally observed in S-1 that this I/Φ ratio was maintained for the duration of a discharge. If the plasma evolved after formation such that the I/Φ ratio deviated too far from an acceptable range, then relaxation oscillations, with the associated precursor oscillations, restored I/Φ to a range commensurate with that theoretically predicted on the basis of a force-free, minimum-energy state equilibrium. The theoretical value of I/Φ, in MA/V sec, based on a classical spherical-boundary spheromak configuration, is $3.581/r_c$, where r_c is the separatrix radius in meters. In an attempt to further understand these phenomena, a magnetic coil system external to the plasma was installed to (1) look for possible toroidal mode structure of the magnetic fluctuations, and (2) monitor the gross behavior of the spheromak plasma (shift/tilt). Long-lived ($\sim$0.5 msec) spheromak plasmas almost completely detached from the flux core were produced. Well-defined modes with an assumed form $e^{i(m\theta + n\phi)}$ are observed almost always during the formation phase, with n in the range 1–5, where θ is the poloidal angle and ϕ is the toroidal angle. These modes are important for two reasons: they can play an important function in the relaxation of these plasmas toward a minimum-energy state; and they probably negatively affect energy and particle confinement.

The important relation of these modes to flux conversion and relaxation during formation and to the evolution of the $q(\Psi)$ profile is demonstrated, where q is the usual "safety factor" of tokamak terminology and Ψ is the poloidal flux. A significant finding is the temporal progression of the magnetohydrodynamic (MHD) activity through an $n = 5, 4, 3, 2$; $m = 1$ mode sequence during formation. This is shown to correspond with the time evolution of the central q through the rational fractions $m/n = 1/5, 1/4, 1/3, 1/2$ to a final value of $\sim$0.7. This progression is analogous to that for magnetic oscillations seen in a tokamak during the startup phase. Experimental and theoretical data suggest that these modes in S-1 are probably internal resistive MHD instabilities originating on rational surfaces in the plasma.

Section II contains a discussion of the experimental de-

 0031-9171/85/123667-09$01.90

tails and the manipulation of the data. Section III describes the behavior of the modes and their relation to the plasma relaxation and the q profile. Section IV contains a summary and conclusions.

II. EXPERIMENTAL APPARATUS AND MAGNETIC PROBE DATA ACQUISITION AND ANALYSIS

The plasma formation in the S-1 type of spheromak device is based on an inductive transfer of toroidal and poloidal magnetic flux from a toroidal "flux core" to the plasma.[15] Figure 1 shows a cross section of the S-1 device displaying the vacuum vessel, equilibrium field coils, flux core, figure-eight stabilization coil system,[20] n-mode diagnostic coil arrays, and plasma. The experimentally obtained contours of constant poloidal flux towards the end of the formation phase wherein the spheromak configuration is not completely detached from the flux core are also shown in Fig. 1.

The formation process proceeds as follows. Initially, a steady-state poloidal equilibrium field is generated to support the final plasma equilibrium. A poloidal field generated by a toroidal current inside the flux core is pulsed on (see Fig. 2, bottom). The superposition of these two fields creates a field weaker on the small-major-radius side of the core. A toroidal solenoid inside the core is then pulsed on at time $t = 0$, and a plasma discharge is initiated. The increasing toroidal flux in this solenoid induces a poloidal current in a toroidally concentric plasma surrounding the core. The associated toroidal field distends the plasma, stretching it toward the device axis where the poloidal field is weakest. Simultaneously, the toroidal current in the core is reduced to induce a toroidal current in the plasma. Magnetic reconnection of the poloidal field occurs and a plasma toroid, the desired spheromak configuration, is created.

The S-1 device has been creating a plasma with a major radius of about 55 cm and a minor radius of about 30 cm.

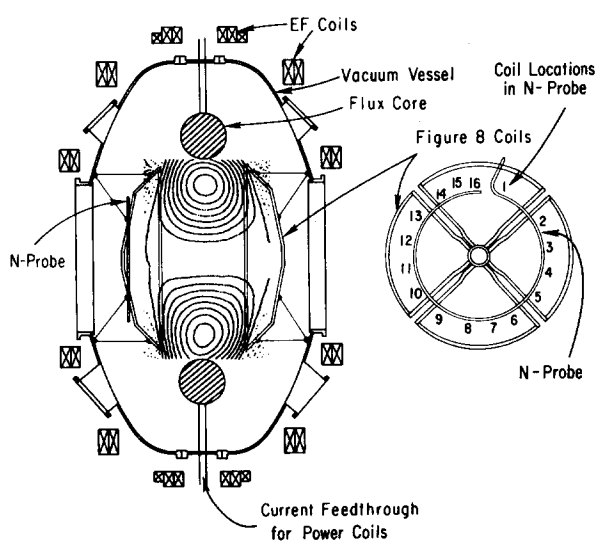

FIG. 1. Cross section of S-1 device showing vacuum vessel, equilibrium field coils, flux core, passive figure-eight stabilization system, and the n-mode diagnostic. The experimentally obtained poloidal flux contours of a spheromak configuration toward the end of the formation phase are also shown.

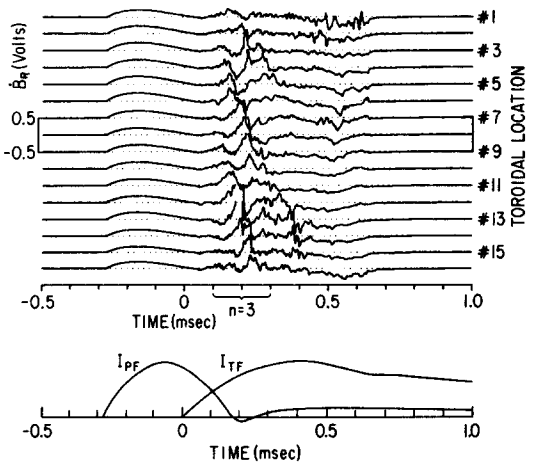

FIG. 2. Time evolution of $\dot{B}_R$ for 16 toroidal angles. An obvious $n = 3$ mode is evident at $t \sim 0.2$ msec, propagating toroidally. Plasma is initiated at $t = 0$.

Toroidal plasma currents up to 350 kA are obtained. Peak plasma electron densities for the discharges reported herein range from 2×10^{13} cm^{-3} to 1×10^{14} cm^{-3}; measured electron temperatures range from 20 to 110 eV, with discharge-averaged temperatures reaching 70 eV.

Stability against rigid-body $n = 1$ modes, provided by a passive figure-eight stabilization coil system,[20] has allowed the formation of spheromaks which are nearly completely detached from the core and are sufficiently stable and long-lived (~ 0.5 msec) to allow the observation of the evolution of $n \geqslant 2$ modes as the plasma forms and decays. The results in this paper cover operation after installation of the figure-eight coils.

Our investigations of the MHD fluctuations have utilized a variety of diagnostic devices. The n-mode diagnostic coil array consists of 16 pairs of magnetic pickup coils distributed toroidally, at equal angles over the full 360°, inside the vacuum vessel at a major radius of $R_0 = 50$ cm and an axial position of $z_0 = 60$ cm (Fig. 1). The coils are located just outside the figure-eight coil system and the figure-eight coil system is, in turn, outside the separatrix of the spheromak magnetic configuration. Each pair of coils measures the time derivative of the magnetic field components in the major radius direction ($\dot{B}_R$) and the toroidal direction ($\dot{B}_\phi$). The coils were designed to measure magnetic field fluctuation levels of 1 G ($\sim 0.1\%$) in a typical frequency range of 5–10 kHz. Coils are comprised of 50 turns with diameters of 0.77 cm (B_R) and 0.60 cm (B_ϕ). The high-frequency cutoff of this coil system is 80 kHz, and at 200 kHz the signals are attenuated by a factor of approximately 2.5. An example of the $\dot{B}_R(t)$ data from the 16-channel array is shown in Fig. 2.

Globally coherent fluctuations, or modes, are often evident from the plot of the 16 channels of $\dot{B}$ vs time. When one mode is predominant, its n number can be determined simply by counting the number of maxima in $\dot{B}$ appearing in the 16 channels at an instant of time, as can be seen in Fig. 2.

The $\dot{B}$ data are digitally integrated to obtain the magnetic fields as a function of toroidal angle ϕ and time t. These fields are then resolved into toroidal n modes by use of discrete Fourier transformation[21] as follows:

$$B(\phi_k,t) = \sum_{n=0}^{N-1} B_n(t) e^{in\phi_k} \tag{1}$$

and

$$B_n(t) = \frac{1}{N} \sum_{k=0}^{N-1} B(\phi_k,t) e^{-in\phi_k} \equiv c_n e^{i\alpha_n}, \tag{2}$$

where $\phi_k = 2\pi k/N$, N is the number of coils (= 16), and k labels each coil. Considering the relation $B_{N-n} = B_n^*$, the amplitude of mode n is

$$\left.\begin{matrix} 2c_n \\ c_0 \\ c_8 \end{matrix}\right\} \text{for } n = \begin{cases} 1,2,\ldots,7, \\ 0, \\ 8, \end{cases}$$

and this is plotted versus time.

The q value is the reciprocal of the rotational transform, $\iota = 2\pi/q$, and is conveniently calculated from $q \equiv d\Phi/d\Psi$, where Φ and Ψ are toroidal and poloidal fluxes, respectively. The time evolution of the $q(\Psi)$ profiles is experimentally determined as follows. The magnetic configuration is measured as a function of space and time, with a movable multicoil magnetic probe inserted into the plasma. The time evolution of a magnetic field profile in major radius, R, is obtained during a single discharge for fixed z (distance along device axis) and ϕ. A two-dimensional cross section of the plasma in a chosen R-z plane is then obtained by scanning this probe in the z direction between discharges. This plot requires data from approximately 40 consecutive and reproducible discharges. This yields a (R,z,ϕ,t) data array with spatial mesh size of 7.5–15 cm. Next, B_z and B_ϕ data are interpolated to produce a finer mesh. The poloidal flux function $\Psi = \int_0^R B_z 2\pi R\, dR$ is then calculated to determine the contours of constant Ψ, and the toroidal flux Φ enclosed by a constant Ψ surface is calculated. Figure 1 shows an example of the contours of constant poloidal flux in the R-z plane. The $q(\Psi)$ profile is obtained from $q(\Psi) = \Delta\Phi/\Delta\Psi$, where $\Delta\Phi$ is the difference in toroidal flux between two nearby surfaces Ψ and $\Psi + \Delta\Psi$.

Other diagnostic devices used to observe fluctuations include an ultrasoft (> 10 eV) x-ray detection system[22] to measure emissivity profiles. An array comprised of 19 silicon surface-barrier detectors views perpendicular to the midplane, with the individual detectors viewing along chords at different major radii distances from the device axis. Also, a triple Langmuir probe is used to measure, at the plasma edge, time-resolved electron density and temperture.

III. DISCUSSION

A. Properties of measured modes

Well-defined modes of low n number ($1 \leqslant n \leqslant 5$) are typically observed during formation from both the B_R and B_ϕ coils, and the B_R and B_ϕ data agree with respect to modes and their evolution. Since the n-mode diagnostic coils are outside the magnetic separatrix of the spheromak configuration, the toroidal field signals cannot be due to poloidal plasma currents. Instead, these modes must be associated with some helical deformation which generates a toroidal component of B from the unperturbed axisymmetric poloidal field.

The larger amplitude modes are easily seen on the $\dot{B}$ data, and sometimes even on the integrated B data, as disturbances periodic in ϕ with an integer number of periods around the torus. An example of $\dot{B}_R$ data exhibiting a well-defined $n = 3$ mode is shown in Fig. 2. The $n = 3$ mode is evident between $t = 0.15$ and 0.25 msec and is seen to be propagating in the direction of increasing "toroidal location number." Time $t = 0$ indicates the initiation of the plasma discharge. The signal before $t = 0$ is due to the pulsed poloidal vacuum field.

Fourier analysis of these fluctuations shows that these are well-defined modes with activity levels peaking midway through the formation phase and sometimes lasting into the post-formation phase. An example of this for a different discharge from above is shown in Fig. 3. There is usually one dominant mode present at a time, and it has an amplitude well above (up to 20 times) the "background" level. Typical mode amplitudes are 5–10 times the background level. The low-level background amplitude shows no clear evolution through a discharge. The imperfect alignment of the figure-eight coils causes currents to be generated in them not only from the rise of the vacuum poloidal field but also from the axisymmetric formation of the spheromak discharge. This is the largest source of the background. For the discharge in Fig. 2, the peak amplitude of the $n = 3$ mode is 20 times the background level.

Figure 3 represents a typical experimental measurement of the time evolution of mode amplitudes. In this case, an $n = 3$ mode starts developing at ~ 0.1 msec into the dis-

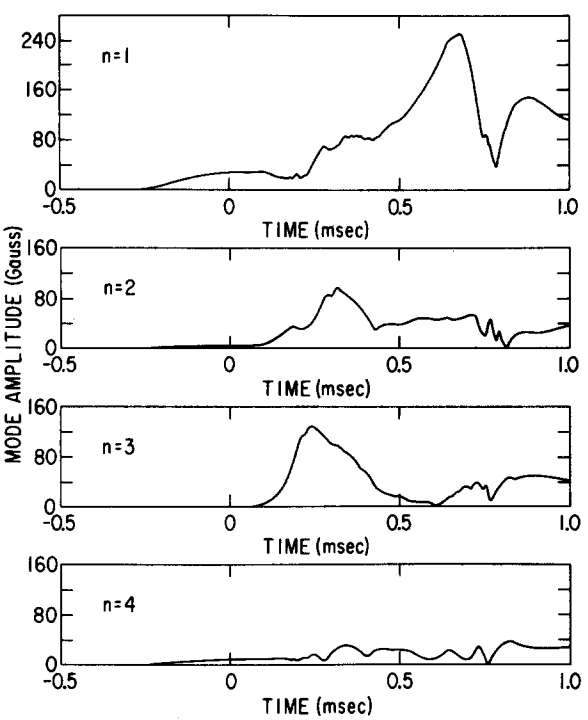

FIG. 3. Mode amplitude versus time for modes $n = 1, 2, 3, 4$. This discharge shows a clear sequential time evolution of the n modes. During the rise of the vacuum poloidal field prior to $t = 0$, the B_R system picks up $n > 0$ components of B_R in addition to the expected large $n = 0$ component. These are due to currents induced in the figure-eight coils because of a slight misalignment with respect to the flux core.

charge, reaches its half-maximum at 0.18 msec and its peak at 0.24 msec, decays to half-maximum at 0.38 msec, and disappears by 0.45 msec. An $n = 2$ mode undergoes similar evolution, peaking at 0.32 msec. In this case, the formation phase is completed by 0.4 msec, and the discharge terminates at approximately 0.75 msec.

The $n = 0$ component of the measured B_R fields, which is primarily comprised of the unperturbed axisymmetric poloidal field of the spheromak configuration, is on the order of 0.5–1.0 kG, comparable to the peak toroidal and poloidal fields measured with magnetic probes internal to the plasma. Peak amplitudes of the $n = 2$, 3, 4 modes relative to the unperturbed field have been observed as high as 20%. More typical amplitudes are below 5%. After formation, amplitudes are less than 1%. These amplitudes are similar to those observed in magnetized-coaxial-gun generated spheromaks after injection into flux conservers.[13,23]

The $n = 1$ mode is associated with a shift or tilt of the plasma and leads ultimately to the termination of the discharge for well-detached plasmas. The $n = 2$ mode often rotates; the $n = 3$ and 4 modes almost always rotate. The rotation is always in the electron diamagnetic drift direction V_{D_e}, which is the same as the direction of propagation of magnetic field fluctuations observed in tokamaks.[24] The modes in S-1 have been observed to rotate at velocities ranging from 0.12 to 1.2×10^6 cm/sec, approximately an order of magnitude slower than the Alfvén velocity. Occasionally, two modes are present simultaneously, and it is observed that these two modes can have rotation velocities differing by as much as a factor of three. This implies that mode rotation is not associated with a rigid-body rotation of the plasma. Also, the rotation velocity often slows with time, indicating a possible dependence of the rotation velocity on magnetic field, electron density, or electron temperature.

Mode structures often do not make much more than one full toroidal rotation before diminishing or changing into another mode structure. Therefore, the growth and decay times of a mode are often on the same time scale as a period of revolution ($\sim$0.1 msec), while being much shorter than the discharge time. Nevertheless, a dominant magnetic-field-fluctuation frequency is easily read from the raw data or the Fourier-analyzed data when a mode is present. Observed frequencies range from 2 to 10 kHz and above.

At any given instant in time (or if the modes were stationary in space), the information from the $N = 16$ coils can be used to identify magnetic structures with mode numbers $n = N/2 = 8$ or less. These measurements may identify actual modes with number $n \leqslant 8$, or, because of aliasing, undetectable high n-number modes ($n > 8$) may show up as false low n-number modes. Aliasing is not considered a problem in these experiments since modes with $6 \leqslant n \leqslant 8$ have amplitudes which are almost always negligible compared to those of modes with $n \leqslant 5$.

It is, therefore, not as likely that modes with $n > 8$ have significant amplitudes in the present experiment compared to the possible situations where modes with $6 \leqslant n \leqslant 8$ have significant amplitudes. Also, all the modes are observed to rotate toroidally in the same direction. This additional information can be used to identify modes with numbers $9 \leqslant n \leqslant 16$ from those with $0 \leqslant n \leqslant 8$. It is found that modes with numbers $9 \leqslant n \leqslant 16$ are small and thus can be eliminated as possible candidates for aliasing. Also, since modes with n numbers in the range $n = 6$–8 (and often $n = 4$ and 5) usually have small amplitudes, modes which can alias with these can be eliminated as having significant amplitudes. That is, modes with numbers $n = 22$–26 (and often $n = 20$, 21, 27, 28) probably have small amplitudes. If so many modes with high n numbers have small amplitudes, it would be fortuitous that the intermediate modes, with numbers $17 \leqslant n \leqslant 19$, have high amplitudes. Lastly, theory predicts that the lower n modes are more unstable. Thus, below $n = 29$, only modes with $n \leqslant 4$ or 5 have significant amplitudes, and the measurements and results are not affected by aliasing problems.

It should be stressed that the above-described modes are prevalent during formation and shortly thereafter. The MHD activity in the post-formation phase does not show such large-amplitude global fluctuations with the n-mode diagnostic system. However, in addition to the above-described modes, there are fluctuations which are locally but not globally coherent in ϕ with frequencies of 100 – 200 kHz. Amplitudes of these high-frequency fluctuations are also on the order of $\tilde{B}/B \lesssim 5\%$. These fluctuations seem to be correlated between up to five or six adjacent coils, and are therefore localized in toroidal angles of 100° or less. High-frequency fluctuations have also been observed earlier[18,19] on the total toroidal plasma current and total magnetic flux in the plasma. Whereas the fluctuation levels on the total current and flux were high only during formation, the levels measured by these local pickup coils persist throughout the discharge. High-frequency fluctuations are also observed in other local measurements such as electron density, measured with Langmuir probes, and in line-integrated measurements such as ultrasoft x ray. These spatially localized fluctuations may be high n-number "modes" which do not have global coherence because of the large number of modes and the high shear on the edge of the plasma. These will be studied elsewhere.

B. Evolution of modes during formation

The mode numbers which occur and the mode amplitudes are very dependent on the programming of the formation process. For typical operating conditions, modes $n = 2$ and 3 occur most often.

A significant finding is the observation of a temporal progression through the $n = 5, 4, 3, 2$ mode sequence during formation. Sequences are almost always from high n to lower n. The nth mode is usually decaying while the $(n-1)$th mode is growing. Figure 3 shows a typical time progression through a $n = 3, 2, 1$ mode sequence. Figure 4 shows the time evolution of the nth component of $B_R(\phi)$ from the Fourier analysis for $n = 1$–4. The well-defined mode structures are evident. Higher n-mode lobes are often observed to develop into lobes of the lower n-mode structures.

The relative weakness of the $n \geqslant 4$ modes may be in part attributable to their development earlier in the formation process and, therefore, their further distance from the magnetic coils. Occasionally, however, a strong, well-defined $n = 4$ or 5 mode does appear.

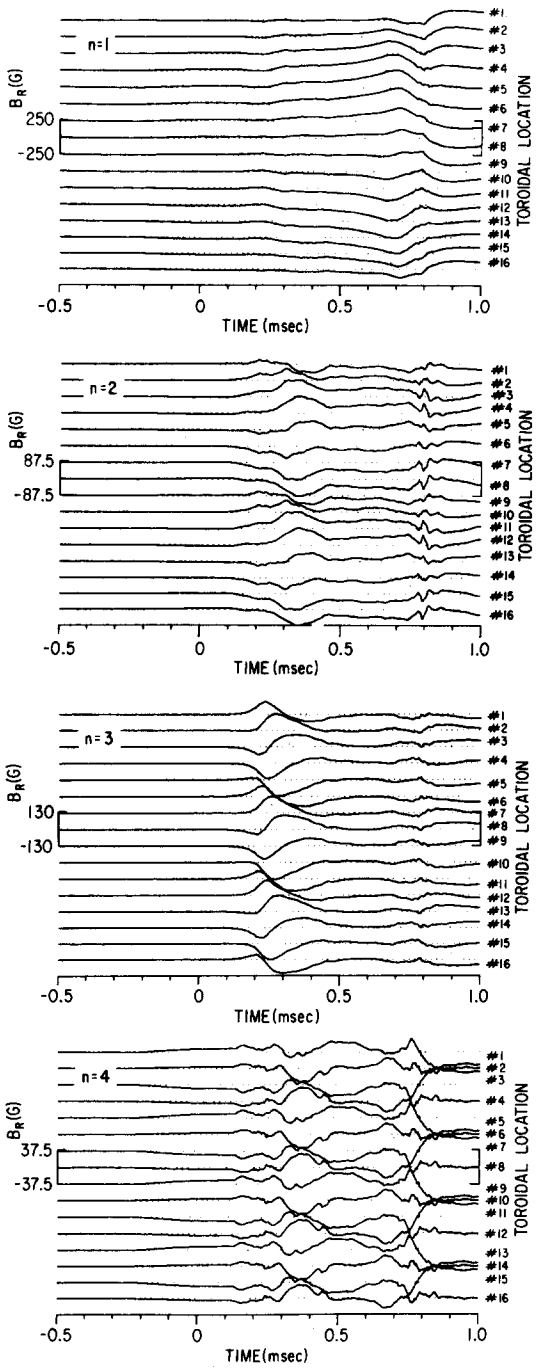

FIG. 4. Time evolution of the nth component of B_R for 16 toroidal angles for $n = 1$–4. This is the same discharge as in Fig. 3.

The plasma always survives the $n > 1$ modes. Only the $n = 1$ leads to termination for well-detached plasmas, if the plasma does not simply decay away before shifting and/or tilting.

C. Mode evolution and q profiles

This temporal progression of modes is reminiscent of that for the magnetic oscillations observed [25] during the start-up phase of a tokamak plasma as early as the 1970's. In the tokamak case, a progression of $m = 6, 5, 4, 3, 2$; $n = 1$ modes is observed as $q(\Psi)$ decreases and $q = m/n$ rational

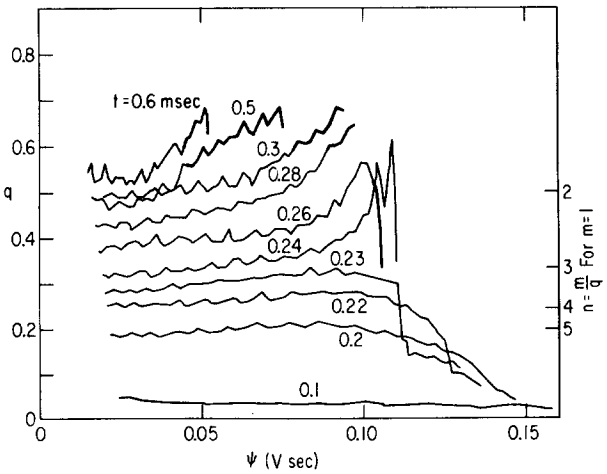

FIG. 5. Plots of $q(\Psi)$ vs time.

surfaces enter the plasma. These modes rotate in the electron diamagnetic drift direction and are now believed to be due to tearing modes.[26,27] For the spheromak case, comparison of the time evolution of the $q(\Psi)$ profile with that of the modes also shows a close relationship.

Figure 5 represents the time evolution of $q(\Psi)$ vs Ψ derived from flux plots such as the one shown in Fig. 1. These flux plots represent an average behavior over many discharges and, therefore, the modes are not evident on them. The right-hand side of each $q(\Psi)$ curve represents the magnetic axis (peak Ψ). The left-hand sides are not continued to $\Psi = 0$ (major axis of the spheromak) due to increasing uncertainty in the computation of q as magnetic surfaces begin to extend beyond the measured range. The q value at the magnetic axis, q_0, is observed to rise through the rational fractions 1/5, 1/4, 1/3, 1/2, midway through the formation phase. The temporal evolution of the modes described earlier follows a sequence of $n = 5, 4, 3, 2$; $m = 1$ during the precise time interval q_0 is rising through $q_0 = m/n$ values, where $n = 5, 4, 3, 2$; $m = 1$. Once $q_0 > m/n$, the m/n rational surface is inside the plasma.

It is interesting to compare the experimental observations to expectations from resistive stability analysis[28–30] of various spheromak equilibria. The experimentally observed temporal sequence of unstable modes agrees with the analysis of DeLucia *et al.*[28] Figure 6 shows the linear growth rate contours in the continuous space formed by nq_0 and na/R from their work, where a and R are the minor and major radii of the spheromak. This figure corresponds to $m = 1$ perturbations. A straight line from the origin represents one possible equilibrium. The two lines with time labels t_1 and t_2 represent two experimental equilibria during the magnetically active period of spheromak formation, with $t_2 > t_1$. For the t_1 curve, modes with $n = 3$ and higher are resistive MHD unstable, while the $n = 2$ mode is stable. At this time (fixed q profile), the modes are more unstable as n becomes higher. It is suggested that the $n = 3$ mode is predominant at this time t_1 because, according to theoretical predictions,[30] the higher n modes ($n > 4$) nonlinearly saturate at low amplitudes. At the later time t_2, the $n = 2$ mode also becomes resistive MHD unstable. Since the $n = 2$ mode is expected to saturate

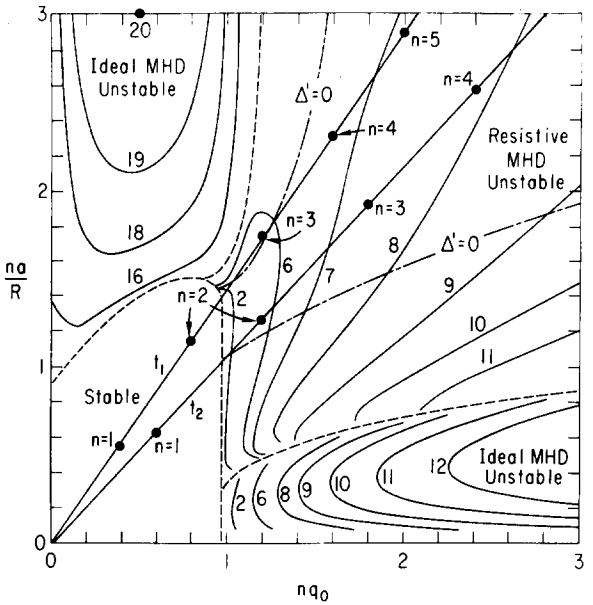

FIG. 6. Growth rate contours in the continuous space formed by nq_0 and na/R. Growth rates are proportional to the integer labels. Stable, ideal MHD unstable, and resistive MHD unstable regions are distinguished by dashed curves. An equilibrium is represented by a straight line starting at the origin. Typical experimental equilibria during the period of strong mode activity are indicated at times t_1 and t_2 with $t_2 > t_1$.

at a relatively large amplitude compared to higher n modes, and since the $q = m/n = 1/3$ surface for the $n = 3$ mode moves to the edge of the plasma, one might expect the $n = 2$ mode to become strong at this later time t_2. It is of additional interest that the experimental equilibria after formation are never far from the least unstable configuration with $q_0R/a \sim 0.67$. It thus appears that these modes are due to internal resistive MHD instabilities.

Although the plasma in the experiment has a finite aspect ratio, the results from this cylindrical model theory are expected to be applicable for several reasons. First, the magnetic configuration of the forming spheromak in fact has a relatively large aspect ratio ($\gtrsim 2$), so that a cylindrical approximation is reasonable. Second, toroidal effects on the spheromak resistive stability results are expected[28] to be small since the toroidal current density, and temperature, should peak near the magnetic axis where the flux surfaces are nearly circular. Also, since $q < 1$ everywhere, poloidal curvature will always be dominant over toroidal curvature. Since the toroidal magnetic field in a spheromak is weak compared to that in a tokamak, toroidal curvature effects are expected to be small in comparison. Third, resistive MHD results depend on whether rational surfaces exist in the plasma; if they do, then the consequences are expected to be similar whether one is using a cylindrical or a toroidal model. With regard to ideal MHD stability, a comparison made between results from cylindrical and toroidal treatments[29] showed similar results.

There is good evidence that the poloidal mode structure of these fluctuations is $m = 1$. First, a dominant $m = 1$ mode structure is observed with the ultrasoft x-ray system during the time period of strong magnetic mode activity. Second, theoretical analysis[28] indicates that the $m = 1$ modes are most unstable.

Looking at $q(\Psi)$ in more detail, $q(\Psi)$ is zero at the start of the discharge due to the purely poloidal field configuration in vacuum. During the early part of the formation before flux surfaces detach from the core ($t < 0.24$ msec), q rises away from the magnetic axis. Magnetic reconnection occurs after 0.24 msec, allowing the formation of detached flux surfaces. Also, the basic shape of the $q(\Psi)$ profile changes from one with a minimum at the magnetic axis before reconnection to one which is an increasing function of Ψ after reconnection starts. After formation ($t > 0.4$ msec), $q(\Psi)$ is a monotonically increasing function of Ψ from the separatrix ($R \simeq \pm 80$ cm) to $q_0 \simeq 0.73$ at the magnetic axis ($R \simeq \pm 60$ cm). This general profile is then maintained for the remainder of the discharge. For comparison, the classical spherical-boundary spheromak configuration[2] has $q_0 = 0.82$, with q monotonically decreasing to $q_s = 0.72$ on the separatrix; a classical spheromak with the same degree of oblateness as the experimental configuration has a q_0 of 0.65, with q decreasing to 0.47 at the separatrix. The time evolution of modes is not shown for the discharges used in the calculation of $q(\Psi)$; however, there is sharp peaking of mode activity between 0.15 and 0.25 msec, with strong $n = 3$ and $n = 2$ components present. Both modes are often simultaneously at or above their half-maximum amplitude at some instant during the formation phase, leading to possible mode interaction. These modes and the effects of possible interaction between these modes, together with reconnection, probably help to change the shape of the $q(\Psi)$ profile.

D. Plasma relaxation

It has been reported earlier[18,19] that flux conversion is a strong mechanism during spheromak formation in the S-1 Spheromak. There are several indications that the modes described above play a crucial role in the relaxation of the spheromak toward a minimum-energy state.[4]

Both these modes and the relaxation are most prevalent during formation. In some cases, the applied coil currents would be expected to produce an equilibrium far from the Taylor state if the fluxes were transferred directly into the plasma. However, there is observed to be conversion of poloidal flux into toroidal flux or vice versa during formation. The plasma adjusts itself during formation to achieve a constant ratio between the poloidal and toroidal fluxes ($I/\Phi \propto \lambda = \text{const}$), independent of initial conditions. The data show a final equilibrium near the Taylor force-free, minimum-energy state. The q-profile evolution described above also suggests a relaxation.

A time evolution of the inventory of poloidal and toroidal fluxes shows that there is a sudden (relative to the formation time) and large exchange of fluxes during the period of strong mode activity midway through the formation; thereafter, a quiescent equilibrium is achieved. For the example to be described below, the poloidal flux captured by the spheromak is seen to drop precipitously during the same period that there is a sudden and large increase in the toroidal flux in the plasma. Figure 7 shows the time evolution of the poloidal and toroidal fluxes measured from the two-dimensional flux plots described above. Figure 7(a) shows the maximum po-

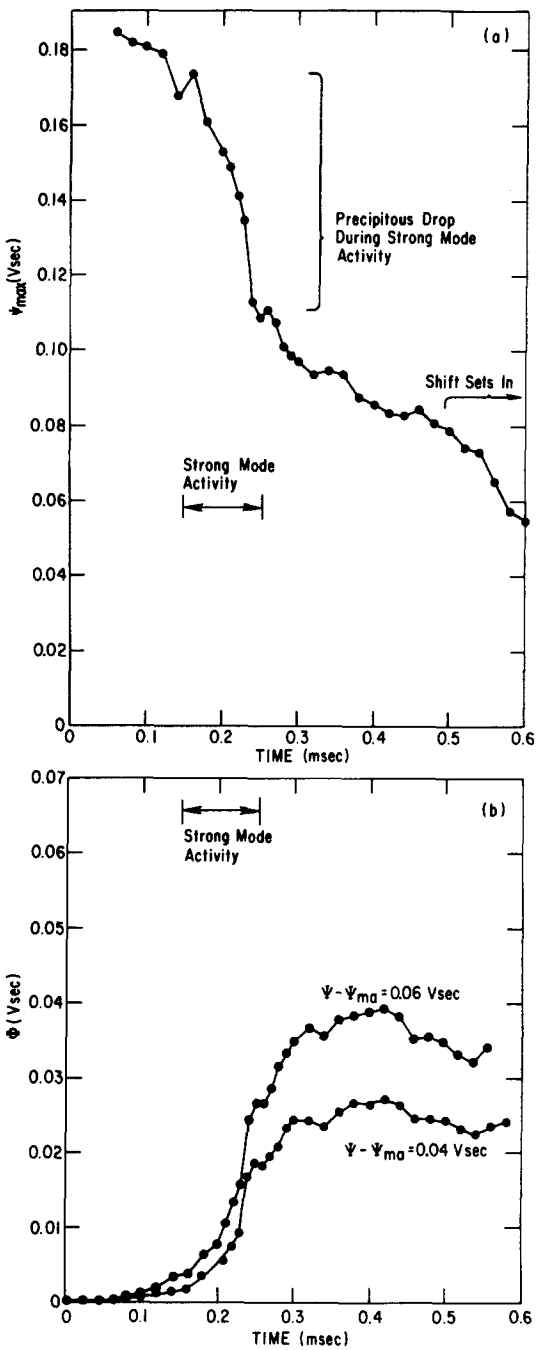

FIG. 7. Time evolution of (a) maximum poloidal flux Ψ_{max} and (b) toroidal flux Φ included in the poloidal flux contour a distance $|\Psi - \Psi_{max}|$ from Ψ_{max}. There is a precipitous drop in Ψ_{max} and a concurrent sudden and large increase in Φ during the period of strong magnetic mode activity.

loidal flux Ψ_{max} defined by the integral $\int 2\pi R B_z \, dR$ from $R = 0$ to $R = R_{max}$, where R is major radius and R_{max} is R at the magnetic axis if there is one; otherwise R_{max} is the inside major radius of the flux core. Each of the curves in Fig. 7(b) is the measured toroidal flux within a closed poloidal flux surface defined by a constant poloidal flux distance $|\Psi - \Psi_{max}|$ from Ψ_{max}. The $|\Psi - \Psi_{max}| = 0.06$ V sec curve includes over 50% of the total toroidal flux. Comparison of Φ curves for different $|\Psi - \Psi_{max}|$ reveals that toroidal flux is increased throughout the plasma and especially deep within the configuration (small $|\Psi - \Psi_{max}|$). It would be interesting to compare these results with a theoretical determination of the profile of the redistributed flux as a consequence of different instabilities, but this information apparently does not yet exist. As was stated above, there is a sharp peaking of $n = 3$ and 2 mode activity between $t = 0.15$ and 0.25 msec. It is precisely during this ~0.1 msec time period that the fluxes undergo dramatic changes. The peak poloidal flux drops by approximately 35% (~0.06 V sec) as the toroidal flux increases by more than a factor of 6 (~0.025 V sec). This behavior is interpreted as relaxation toward a lower energy state. The final magnetic equilibrium was recently[31] shown to be one which has relaxed close to the Taylor state by measuring the λ profile over the two-dimensional minor cross section of the plasma and discovering that it was independent of position except at the plasma edge. The formation phase in these discharges is completed by 0.4 msec.

After formation is complete, the poloidal flux is observed to decay slowly due to resistive losses. The toroidal flux is also observed to decay, but at a slower rate. This difference in decay rates may be due to a continuous low level of flux conversion during the decay phase.

IV. SUMMARY AND CONCLUSIONS

We have shown strong evidence that low n-number modes play an essential role in relaxation of the S-1 Spheromak plasma toward the Taylor state during formation, wherein there can be a large transfer of magnetic flux. The temporal evolution of modes through the $n = 5, 4, 3, 2$; $m = 1$ sequence parallels the rise of the experimentally measured q_0 through m/n rational fractions. This is analogous to the evolution of magnetic oscillations observed during the startup phase of a tokamak plasma in which a progression of $m = 6, 5, 4, 3, 2$; $n = 1$ modes is observed as q decreases and $q = m/n$ rational surfaces enter the plasma. Experimental observations and comparison of theoretical predictions with experiment suggest that the modes observed in S-1 are probably resonant modes due to resistive MHD instabilities.

This progression caused by the $q(\Psi)$-profile evolution distinguishes spheromaks formed by the S-1 induction technique from those formed by magnetized coaxial guns. In the latter case the $q(\Psi)$ profile begins with q high, after which q falls, so that a different progression of modes might be expected. In fact, such gun-generated spheromaks have been observed to display large $n = 1$ and 2 activity. Results from CTX[13] show that coherent, rigidly rotating $n = 1$ and $n = 2$ modes are generated during the sustained and decaying phases of the discharge, respectively. According to ideal MHD,[32] these modes are nonresonant, but the $n = 2$ appears when q is just below 0.5.

The modes observed in S-1 are expected to affect energy confinement. In tokamaks, the energy confinement time decreases as mode amplitudes become large ($\simeq$1%). It is observed[27] in tokamaks that strong disruptions in the current rise phase can degrade the plasma quality throughout the remainder of the discharge; proper programming of the rate of current rise avoids these disruptions. A carefully programmed formation in spheromaks may minimize the bad

effects of these modes. The effects of these modes in S-1 on plasma parameters have yet to be investigated in detail.

ACKNOWLEDGMENTS

The authors thank S. Jardin for relating his extensive theoretical results to these experimental observations and R. Ellis, Jr. for his thorough review of this research and very useful discussion. This work was supported by U.S. Department of Energy Contract No. DE-AC02-76-CHO-3073.

APPENDIX: ERRORS IN THE CALCULATION OF q

Early in the discharge ($t < 0.24$ msec), there are no flux surfaces which are detached from the core (that is, which do not encircle the flux core). The q function is numerically calculated, nevertheless, using data for which $|R| \leqslant 80$ cm. A systematic error in the calculated q is incurred because the toroidal flux beyond $|R| = 80$ cm is not measured. This systematic error in q is expected to be small for not too small Ψ, and to increase as Ψ decreases. With regard to this systematic error, the calculated q is always a lower limit of the actual q. A rough estimate of a typical deviation of the true q from that calculated, due to this system error, is $+0.1$ at small Ψ ($\Psi \approx 0.02$ V sec) for $t \approx 0.3$ msec. As flux surfaces detach from the core, the portion of the $q(\Psi)$ curve corresponding to these surfaces is indicated by bold lines.

Another possible source of error in the axisymmetric analysis used to determine $q(\Psi)$ is the existence of nonaxisymmetric modes. This, however, is not expected to affect the results for several reasons.

First, the deviations are small (typically $\lesssim 5\%$) so that the assumption of axisymmetry is not bad for data from a given discharge.

Second, the flux plots are derived from many ($\simeq 40$), fairly reproducible (to within 5%), plasma discharges because the one-dimensional probe array must be moved between discharges to obtain a two-dimensional flux plot, and because an average over several discharges is made at any given spatial position. Although there is quantitative similarity in mode behavior from discharge to discharge (approximate starting time and position, amplitude, duration), there is certainly enough variation among different discharges that mode features would not be visible in the final flux plots. The averaging removes the details of individual discharges, and the flux plots are consequently of the mean fields for which it is valid to calculate q. The q profiles, which are based on these flux plots, will not show details of the modes, and therefore, will not show errors due to the assumption of axisymmetry in the presence of modes. The profiles, however, will show the resulting effects of these modes on the mean fields.

Third, the modes are limited in spatial extent (plasma radius) and in time duration. The assumption of axisymmetry is not questionable except for the perturbed volume during the occurrence of a mode. This "brackets" the possible q values, and the actual rotational transform of a field line near a mode (in space and time) cannot be far from that calculated in the analysis.

Last, the results are not changed for discharges with very small mode amplitudes and, therefore, for discharges whose flux surfaces are minimally perturbed by these low n-number modes. This suggests that reduction of data from discharges with large amplitude modes is not affected by the large amplitudes. The variation in measured magnetic fields from discharge to discharge results in an error of $\pm 10\%$–20% in the calculation of q_0.

[1] H. A. B. Bodin and A. A. Newton, Nucl. Fusion **20**, 1255 (1980).

[2] M. N. Bussac, H. P. Furth, M. Okabayashi, M. N. Rosenbluth, and A. M. M. Todd, in *Plasma Physics and Controlled Nuclear Fusion Research 1978, Proceedings of the Seventh International Conference, Innsbruck, Austria* (IAEA, Vienna, Austria, 1979), Vol. III, p. 249; H. P. Furth, J. Vac. Sci. Technol. **18**, 1073 (1982).

[3] H. Alfvén, L. Lindberg, and P. Mitlid, J. Nucl. Energy, Part C: Plasma Phys. **1**, 116 (1960): L. Lindberg and C. Jacobsen, Astrophys. J. **133**, 1043 (1961).

[4] J. B. Taylor, in *Proceedings of the Third Topical Conference on Pulsed High β Plasmas, IKAEA Culham Laboratory, U.K.*, 1975 (Pergamon, Oxford, 1976), p. 59; J. B. Taylor, Phys. Rev. Lett. **33**, 1130 (1974).

[5] C. A. Bunting, C. W. Gowers, K. Ogawa, D. C. Robinson, and M. R. C. Watts, in *Proceedings of the Eighth European Conference on Controlled Fusion and Plasma Physics 1977, Prague, Czechoslovakia* [(distributed by) Institute of Plasma Physics, Czechoslovakia Academy of Science, Prague, 1977], Vol. 1, p. 79.

[6] D. A. Baker, M. D. Bausman, C. J. Buchenauer, L. C. Burkhardt, G. Chandler, J. N. Dimarco, J. N. Downing, P. R. Forman, R. F. Gribble, A. Haberstich, R. B. Howell, J. C. Ingraham, A. R. Jacobson, F. C. Jahoda, K. A. Klare, E. M. Little, L. W. Mann, R. S. Massey, J. Melton, G. Miller, R. Moses, J. A. Phillips, A. E. Schofield, K. F. Schoenberg, K. S. Thomas, R. G. Watt, P. G. Weber, and R. Wilkins, in *Plasma Physics and Controlled Nuclear Fusion Research 1982, Proceedings of the Ninth International Conference, Baltimore, Maryland* (IAEA, Vienna, Austria, 1983), Vol. I, p. 587.

[7] T. R. Jarboe, I. Henins, A. R. Sherwood, Cris W. Barnes, and H. W. Hoida, Phys. Rev. Lett. **51**, 39 (1983).

[8] I. H. Hutchinson, M. Malacarne, P. Noonan, and D. Brotherton-Ratcliffe, Nucl. Fusion **24**, 59 (1984).

[9] V. Antoni and S. Ortolani, Plasma Phys. **25**, 799 (1983).

[10] T. Tamano, T. Carlstrom, C. Chu, R. Goforth, G. Jackson, R. La Haye, T. Ohkawa, M. Schaffer, P. Taylor, N. Brooks, and R. Chase, in Ref. 6, Vol. I, p. 609.

[11] R. G. Watt and R. A. Nebel, Phys. Fluids **26**, 1168 (1983).

[12] A. R. Sherwood, Bull. Am. Phys. Soc. **28**, 1188 (1983).

[13] B. L. Wright, in *Proceedings of the Sixth U. S. Symposium on Compact Toroid Research and the Fifth U. S.–Japan Joint Symposium on Compact Toroid Research, Princeton, New Jersey, 1984* (Princeton University Plasma Physics Laboratory, Princeton, NJ, 1985), pp. 5–8.

[14] R. S. Shaw, J. Antoniades, C. Chin-Fatt, A. W. DeSilva, G. C. Goldenbaum, and R. Hess, in Ref. 13, pp. 53–56.

[15] M. Yamada, H. P. Furth, W. Hsu, A. Janos, S. Jardin, M. Okabayashi, J. Sinnis, T. H. Stix, and K. Yamazaki, Phys. Rev. Lett. **46**, 188 (1981).

[16] T. Jarboe, I. Henins, H. W. Hoida, R. K. Linford, J. Marshall, D. A. Platts, and A. R. Sherwood, Phys. Rev. Lett. **45**, 1264 (1980).

[17] G. Goldenbaum, J. H. Irby, Y. P. Chong, and G. W. Hart, Phys. Rev. Lett. **44**, 393 (1980).

[18] A. Janos, in Ref. 13, pp. 97–102.

[19] M. Yamada, R. Ellis, Jr., H. P. Furth, G. Hart, A. Janos, S. Jardin, F. Levinton, D. Meyerhofer, M. Mimura, C. H. Nam, S. Paul, A. Sperduti, S. Von Goeler, F. Wysocki, and P. Young, in *Plasma Physics and Controlled Nuclear Fusion Research 1984, Proceedings of the Tenth International Conference, London, UK* (IAEA, Vienna, Austria, 1985), Vol. 2, p. 535.

[20] S. C. Jardin and U. Christensen, Nucl. Fusion **21**, 1665 (1981).

[21] See, for example, R. N. Bracewell, *The Fourier Transform and Its Applications* (McGraw-Hill, New York, 1978), 2nd ed.

[22] S. F. Paul, G. Hart, A. Janos, F. Levinton, D. Meyerhofer, M. Mimura, C. H. Nam, A. Sperduti, S. von Goeler, F. Wysocki, M. Yamada, and P. Young, in *Proceedings of the Sixth U. S.–Japan Joint Symposium on Compact Toroid Research, Hiroshima, Japan, 1984* (Institute for Fusion The-

ory, Hiroshima University, Hiroshima, Japan, 1985), p. 14.
[23]K. Watanabe, Y. Honda, K. Ikegami, M. Nagata, M. Nishikawa, A. Ozaki, N. Satomi, and T. Uyama, in Ref. 13, pp. 29–32.
[24]J. C. Hosea, C. Bobeldijk, and D. J. Grove, in *Plasma Physics and Controlled Nuclear Fusion Research 1970, Proceedings of the Fourth International Conference, Madison, Wisconsin* (IAEA, Vienna, Austria, 1971), Vol. II, pp. 425–440.
[25]S. V. Mirnov and I. B. Semenov, in Ref. 24, p. 401; Sov. J. At. Energy **30**, 22 (1971); Sov. Phys. JETP **33**, 1134 (1971).
[26]L. A. Artsimovich, Nucl. Fusion **12**, 215 (1972).
[27]R. S. Granetz, I. H. Hutchinson, and D. O. Overskei, Nucl. Fusion **19**, 1587 (1979).
[28]J. DeLucia, S. C. Jardin, and A. H. Glasser, Phys. Fluids **27**, 1470 (1984).
[29]S. C. Jardin, Nucl. Fusion **22**, 629 (1982).
[30]J. DeLucia and S. C. Jardin, Phys. Fluids **27**, 1773 (1984); R. B. White, D. A. Monticello, M. N. Rosenbluth, and B. V. Waddel, *ibid.* **20**, 800 (1977).
[31]G. W. Hart, A. Janos, D. D. Meyerhofer, and M. Yamada, submitted to Phys. Fluids.
[32]G. Marklin, in Ref. 13, pp. 88–91.